Available online at www.sciencedirect.com

SciVerse ScienceDirect

Ceramics International 39 (2013) 1547–1554

CERAMICS INTERNATIONAL

www.elsevier.com/locate/ceramint

Mechanical, morphological and dielectric properties of sintered mullite ceramics at two different heating rates prepared from alkaline monophasic salts

M.M.S. Sanad[a], M.M. Rashad[a,*], E.A. Abdel-Aal[a], M.F. El-Shahat[b]

[a]*Central Metallurgical R&D Institute, P.O. Box 87, Helwan, Cairo, Egypt*
[b]*Ain Shams University, Faculty of Science, Cairo, Egypt*

Received 4 April 2012; received in revised form 30 July 2012; accepted 31 July 2012
Available online 17 August 2012

Abstract

The sintering behavior of nanocrystalline orthorhombic mullite powders was investigated. The changes in microstructure, mechanical and dielectric properties with two different heating rates were explained. Microstructural characteristics depending on heating rate were explained at different sintering temperatures. Dielectric properties of prepared mullite nanocomposites were studied to examine the synthesized mullite ceramics as high permittivity materials in the microwave range. It was indicated that a sharp decrease in bulk density was observed at 1600 °C due to the exaggerated growth of mullite grains. Moreover, a maximum hardness value of 4.97 GPa was obtained at 1600 °C with slow heating rate (5 $^{\circ}min^{-1}$). The DC electrical resistivity with a slow heating rate at 1300 °C was approximately three times the value of the mullite sample sintered with a fast heating rate (30 $^{\circ}min^{-1}$). The minimum dielectric loss of about 0.017 at 1.5 GHz was achieved at a sintering temperature of 1500 °C with a slow heating rate.

Keywords: C. Mechanical properties; Heating rate; Microhardness; O-mullite ceramics

1. Introduction

Mullite ($3Al_2O_3 \cdot 2SiO_2$) is an attractive potential engineering ceramic owing to its unique combination of properties such as high melting point (1830 °C), good electrical resistance, good mechanical strength, low thermal expansion coefficient ($4.5 \times 10^{-6}\,K^{-1}$), high strength and high creep resistance at both low and high temperatures, low electric conductivity and low dielectric constant ($\varepsilon = 56.5$ at 1 MHz) as well as good chemical and thermal stability [1–5]. Due to these desirable properties, it has a wide range of applications in structural, chemical, optical, and electrical industries. Hence, understanding the important factors affecting the mechanical and dielectric properties is an area of great interest and necessary for finding further applications. Microstructural and densification characteristics are previously studied for synthesized mullite ceramics from different raw materials or mullite mixed with different oxides [6–23]. In addition, the dielectric properties of sintered mullite ceramics are poorly investigated for different mullite composites [24–27]. In this paper, the effect of heating rate on the mechanical, morphological and dielectric properties of sintered mullite ceramics at different sintering temperatures from 1300 to 1600 °C prepared from alkaline monophasic salts (sodium aluminate and sodium silicate) using the co-precipitation method was studied. The obtained sintered mullite samples were investigated by X-ray diffraction (XRD) and scanning electron microscopy (SEM). Furthermore, the changes in the mechanical and electrical properties of the produced mullite ceramics were evaluated at different sintering temperatures using two levels of heating rate (5 and 30 $^{\circ}min^{-1}$).

*Corresponding author. Tel.: +20 2 25010642; fax: +20 2 25010639.
E-mail address: rashad133@yahoo.com (M.M. Rashad).

0272-8842/$ - see front matter © 2012 Elsevier Ltd and Techna Group S.r.l. All rights reserved.
http://dx.doi.org/10.1016/j.ceramint.2012.07.105

2. Experimental

2.1. Chemicals

All the chemicals used in this study, such as sodium aluminate $NaAlO_2$ Sigma-Aldrich 99.9%, sodium silicate pentahydrate Sigma-Aldrich 99.9%, hydrochloric acid HCl, ADWIC 37%, were of analytical grade. Deionized water was used in the whole work.

2.2. Procedures

Mullite precursors were synthesized by adding dilute hydrochloric acid solution to the mixed solution of sodium aluminate and sodium silicate (stoichiometrically mixed together achieving a $3Al_2O_3{:}2SiO_2$ ratio) and adjusting the pH value to 7. The aqueous suspensions were stirred gently for 15 min to achieve a good homogeneity and to attain a stable pH conditions. The formed gel is then filtered, washed thoroughly with deionized water and dried overnight at 100 °C in the oven. Dried precursors were calcined at 1000 °C for 2 h at rate of 10 °C/min to form mullite nanopowders (12 nm). The annealed mullite precursors were ground in an agate mortar with a pestle. Mullite compacts were prepared by uniaxially dry pressing the powders in a 12 mm diameter steel die at a pressure of 3 t. Pellets were sintered at temperatures in the range of 1300 and 1600 °C for 5 h with two different heating rates of 5 and 30 °min^{-1}, respectively.

2.3. Characterization

X-ray powder diffraction (XRD) was carried out on a model Bruker AXS diffractometer (D8-ADVANCE Germany) with Cu Kα ($\lambda = 1.54056$ Å) radiation, operating at 40 kV and 40 mA. The diffraction data were recorded for 2θ values between 10° and 70° and the scanning rate was 3° min^{-1} (or 0.02°/0.4 sec). Scanning electron microscopy was carried out by a SEM (JEOL-JSM-5410 Japan). The expansion–shrinkage measurements were made using an Adamel Lhormergy 1/128 in apparatus (Instrument SA, Longjumeau). Porosity and density measurements of sintered samples were determined using PORESIZER 9320 V2.08. Microhardness tests were evaluated by means of a Vickers Microhardness Tester, INDENTEC-HWDN-7 Japan (500 g normal load applied for 15 s) as an average of six measurements. An electrometer and DC power supply (Agilent-4339B, USA) were used for electrical resistivity measurements for the experimental studies. A constant DC voltage (V) of about 1.5 V was applied from a battery across the sample. Dielectric properties were measured using a network impedance analyzer (Agilent-E4991A,USA) that is responsible for the generation and reception of signals in the frequency range of 1 MHz to 3 GHz.

3. Results and discussion

3.1. XRD analysis

The effect of sintering temperatures from 1300 to 1600 °C on the phase composition of mullite samples was followed by XRD analysis. Fig. 1 shows the X-ray diffraction patterns of the mullite sample pellets heated at 1600 °C with two heating rates of 5 and 30 °min^{-1}. The results reveal that the peak intensities of mullite ceramics (JCPDS card no. 79-1457) were increased by decreasing the heating rate. Structural parameters like lattice parameter (a), crystallite size (D), strain (ε) and dislocation density (δ) of the mullite samples at different sintering temperatures have been calculated and listed in Table 1. The crystallite size of the formed powders was estimated according to the Scherrer equation,

$$D = 0.90\lambda/\beta\cos\theta \quad (1)$$

where D is the average grain size, λ is the X-ray wavelength, and θ and β are the diffraction angle and full width at half-maximum (FWHM) of an observed peak, respectively. The strongest peak at $2\theta = 26°$ was used to calculate the crystallite size of these nanoparticles. The lattice strain (ε) was calculated using the relation

$$\varepsilon = \beta\cos\theta/4 \quad (2)$$

The value of dislocation density (δ) was calculated using the relation

$$\delta = 15a/\varepsilon D \quad (3)$$

where a is the lattice parameter.

The XRD results showed that the crystallite size (D) of slow heat treated mullite samples ranged from 29.4 nm at 1300 °C to 40.5 nm at 1600 °C. On the other side, the crystallite size of fast heating mullite samples ranged from 27.6 nm at 1300 °C to 34.9 nm at 1600 °C. Furthermore, it was observed that as the crystallite size (D) increased,

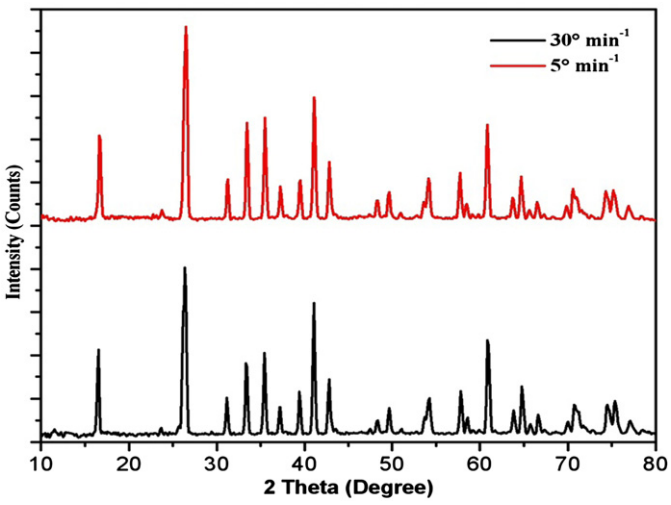

Fig. 1. XRD patterns of mullite samples sintered at 1600 °C for 5 h at various heating rates.

Table 1
Differences between mechanical properties of mullite samples annealed at different heating rates.

Sintering temperature (°C)	a (Å)		C_S (nm)		ε ($\times 10^{-2}$)		δ ($\times 10^{5}$cm^{-3})		H_V (GPa)	
	5 °min^{-1}	30 °min^{-1}	5 °min^{-1}	30 °min^{-1}	5 °min^{-1}	30 °min^{-1}	5 °min^{-1}	30 °min^{-1}	5 °min^{-1}	30 °min^{-1}
1300	7.664	7.656	29.4	27.6	5.47	5.82	7.149	7.149	1.63	1.62
1400	7.660	7.666	32.3	29.1	5.32	5.67	6.687	6.969	2.39	2.29
1500	7.653	7.654	37.2	32.8	4.97	5.11	6.209	6.849	2.59	2.44
1600	7.649	7.650	40.5	34.9	4.63	4.85	6.119	6.779	4.97	4.58

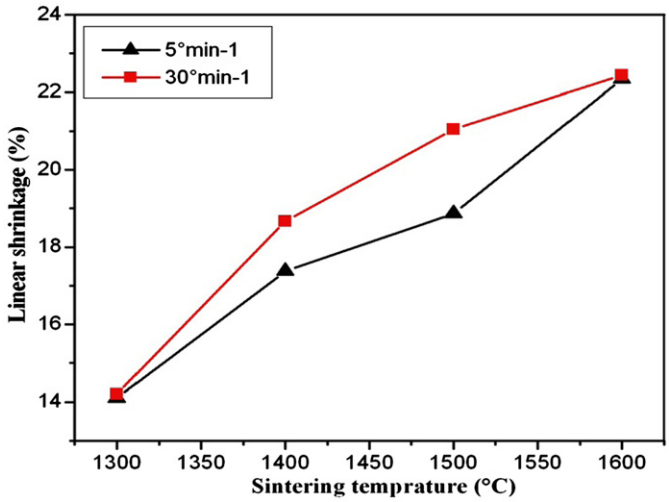

Fig. 2. Effect of heating rate on linear shrinkage of sintered mullite ceramics.

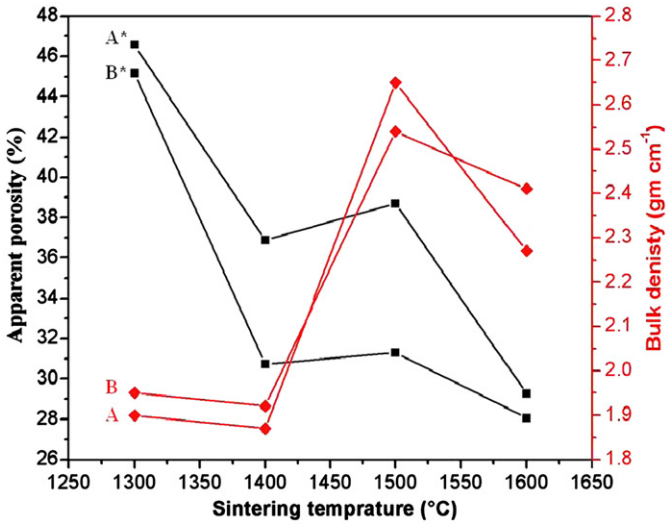

Fig. 3. Effect of heating rate on sintering properties of mullite samples sintered at various temperatures for 5 h. Bulk density and apparent porosity of mullite samples at 5°min^{-1} (A and A*) Bulk density and apparent porosity of mullite samples at 30°min^{-1}(B and B*).

lattice defects decreased, which in turn reduced the internal microstrain (ε) and dislocation density (δ). In fact, the increase in peak intensity and decrease of FWHM were due to improvement in the crystallinity and a reduction in the microstrain [28].

3.2. Sintering and mechanical properties

Fig. 2 shows the change of linear shrinkage of the mullite samples with the heating rate. As the sintering process accelerates with temperature increase, particles get closer, leading to lower porosity, namely higher pellet density. The biggest shrinkage is achieved for samples sintered with fast heating rate, while for those with slow heating rate the shrinkage is much smaller. The variations in bulk density and apparent porosity of mullite samples sintered at two heating rates of 5° and 30° min^{-1} are shown in Fig. 3. It is noticed that the heating rate exhibited a positive effect on the densification of the mullite ceramics. About 19.1% improvement in the density is observed with a 30 °min^{-1} heating rate at the highest sintering temperature under investigation. The apparent porosity was reduced by 4.1% in the rapid heating rate at a sintering temperature of 1600 °C which is in agreement with observations by Li and Li [29]. Furthermore, it was seen that the bulk density of the sample increases with the increasing sintering temperature up to 1500 °C at any rate of heating. Then the maximum densities dropped with rising the temperature up to 1600 °C. The dropping in the bulk density could be related to the formation of short whisker networks, Fig. 3, which act as barriers to densification. In other words, with increasing sintering temperature, the mullite grains grow larger (i.e. exaggerated grain growth) but without shrinkages occurring to promote density [23,30–33]. The mean values of measured microhardness of mullite nanocomposites are depicted in Table 1. It is observed that hardness values increased with rising sintering temperature. In addition, the heating rate affects the hardness values slightly at low sintering temperatures, while strongly affecting the hardness values at high sintering temperature. Such effects could be due to the pronounced difference in porosities and densities of the prepared samples.

3.3. Microstructure investigation

Fig. 4 illustrates the scanning electron microscope (SEM) micrographs of mullite samples sintered at 1300 °C and 1600 °C for 5 h with heating rates of 5° and 30° min^{-1}. As clearly shown, the mullite composites exhibited different

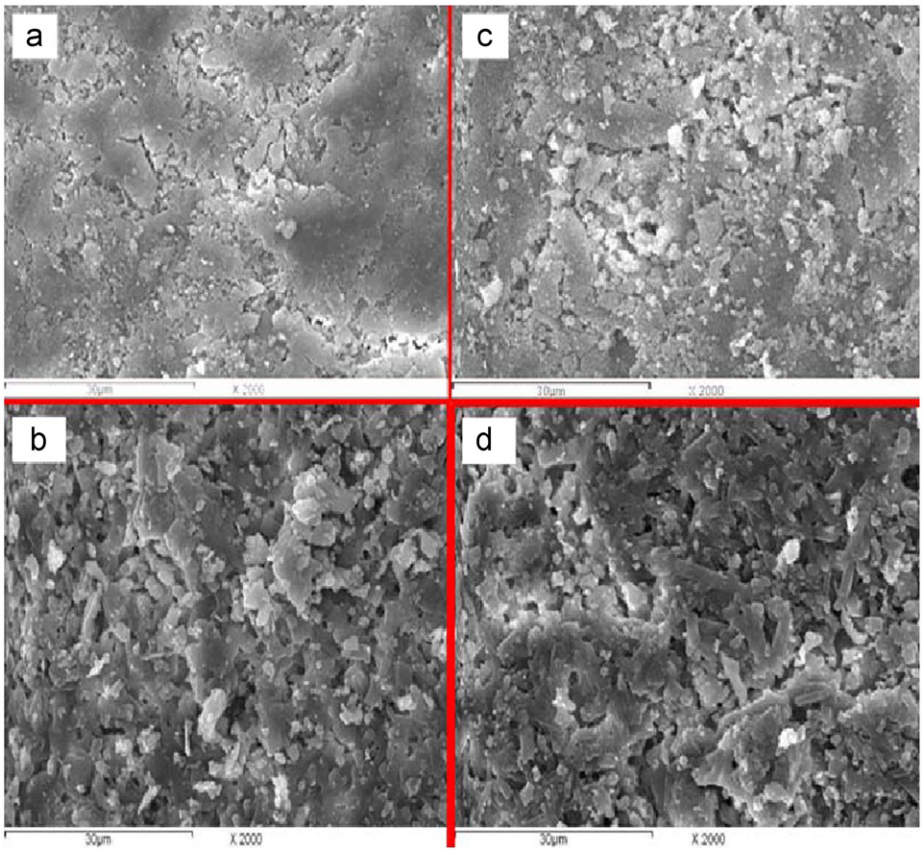

Fig. 4. SEM microstructure of mullite ceramics sintered at 1300 °C and 1600 °C respectively for 5 h. Slow heating rate, 5°min^{-1} (a and b). Fast heating rate, 30°min^{-1} (c and d) [magnification × 2000].

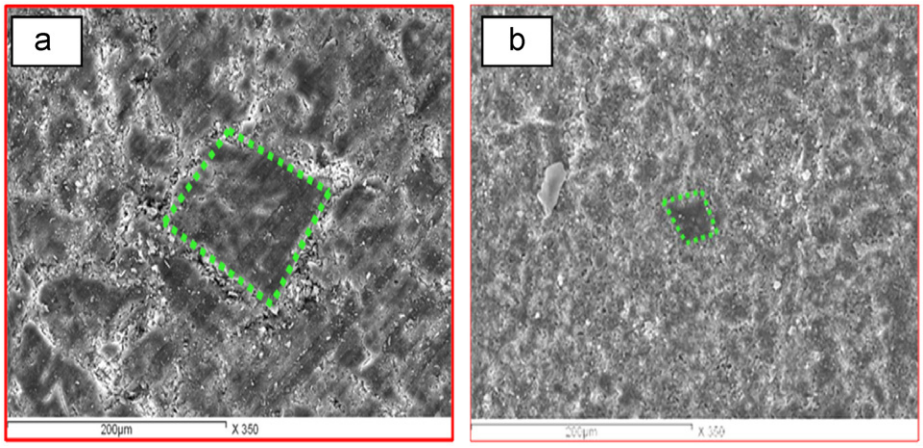

Fig. 5. Typical Knoop or Vicker's impressions of mullite ceramics sintered at 1300 °C (a) and 1600 °C (b), respectively, for 5 h with heating rate 5°min^{-1} [magnification × 350].

microstructure dependences on the heating rate. Microstructure of the mullite composite sintered at 1300 °C with low heating rate (Fig. 4a) was characterized by the formation of agglomerated particles (i.e. higher crystallization) and larger density, while the mullite composites with fast heating rate (Fig. 4c) showed both lower density and agglomeration. On the other hand, microstructures (Fig. 4b and d) of the mullite composites sintered at 1600 °C appeared almost the same but the values of both apparent porosities and bulk densities were totally different [34]. At the same heating rates, sharp growth of mullite grains was observed for mullite samples sintered at 1600 °C (Fig. 4c and d), which may be attributed to the complete crystallization. It was reported that for samples with anisotropic mullite grains, elongated mullite grains were always accompanied with a number of fine mullite grains, and with increasing sintering temperature or time, in the

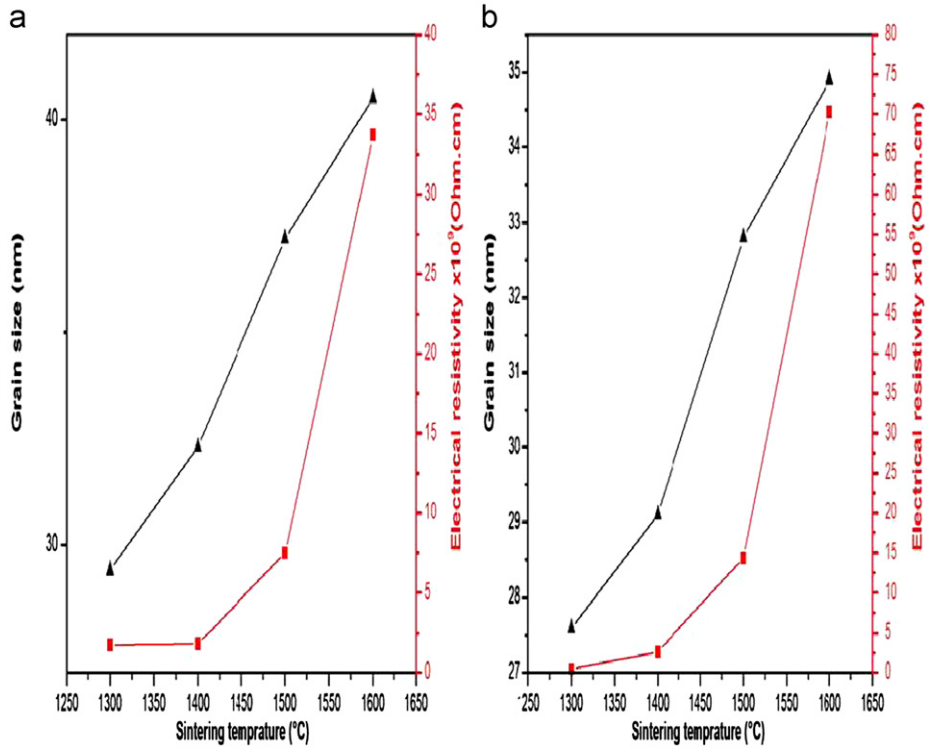

Fig. 6. Correlation between grain size and electrical resistivity of sintered mullite ceramics at various heating rates: (a) 5 °min^{-1} and (b) 30 °min^{-1}.

more elongated grains less fine grains can be formed which is in agreement with the obtained results [35–37].

Fig. 5 depicts SEM micrographs of the impressions obtained by the Knoop or Vickers indentation of mullite samples sintered at 1300 °C and 1600 °C with the same heating rate. As listed in Table 1, it is found that the crack radials in case of higher sintering temperatures were smaller than those of lower sintering temperature. These indenter observations emphasize the rightness of the measured porosities, densities and hardness values.

Table 2
Effect of heating rate on DC electrical resistivity of mullite samples.

Sintering temperature (°C)	ρ (Ω cm)	
	5 °min^{-1} ($\times 10^9$)	30 °min^{-1} ($\times 10^9$)
1300	1.716853	0.453312
1400	1.801799	2.60572
1500	7.44716	14.3391
1600	33.6898	70.2589

3.4. Electrical properties

3.4.1. DC electrical resistivity of sintered mullite

The electrical resistivity (ρ) of mullite samples increases with rising sintering temperature as a result of the densification effect. It is known that in ceramic materials, the absence of lattice defects such as vacancies and interstitials in the structure aids resistance and vice versa [38] as illustrated in Table 2. Consequently, it is found that mullite samples sintered at a fast rate (30° min^{-1}) possess higher electrical resistivity (ρ) values than those samples sintered at a slow rate (5° min^{-1}) within the temperature range of 1400–1600 °C. (Fig. 6) displays the correlation between the grain size (D) and electrical resistivity(ρ) at different sintering temperatures. It is noticeable that both the grain size (D) and electrical resistivity (ρ) were found to increase with increasing sintering temperature of mullite samples.

3.4.2. Dielectric permittivity and dielectric loss tangent of sintered mullite

The dielectric properties of materials are used to describe electrical energy storage, dissipation and energy transfer. Electrical storage is the result of dielectric polarization. Dielectric polarization causes charge displacement or rearrangement of molecular dipoles. Electrical energy dissipation or loss results from electrical charge transport or conduction, dielectric relaxation, resonant transitions and nonlinear dielectric effects.

The plots of dielectric permittivity ($\acute{\varepsilon}$) versus frequency values (Hz) of sintered mullite samples with different heating rates are given in Fig. 7. In general, the values of dielectric permittivity ($\acute{\varepsilon}$) when rapidly heat treated are higher than those values of the slowly heat treated samples. The obvious shift in dielectric permittivity ($\acute{\varepsilon}$) values is coherently accompanied by the obtained bulk density curves.

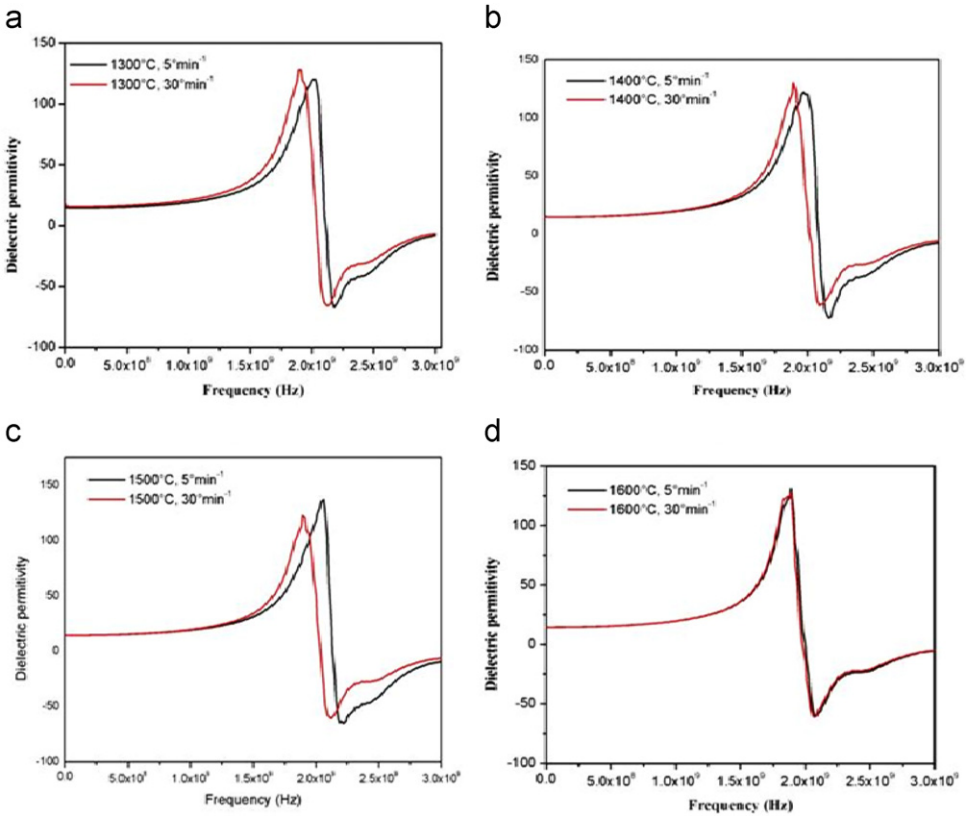

Fig. 7. Dependence of dielectric permittivity ($\acute{\varepsilon}$) of mullite samples on heating rate sintered at (a) 1300 °C (b) 1400 °C (c) 1500 °C and (d) 1600 °C.

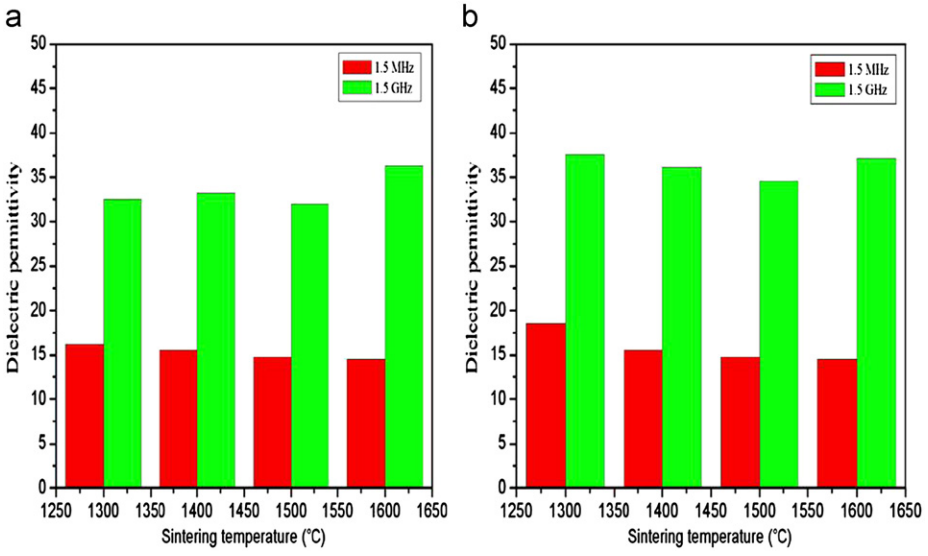

Fig. 8. Effect of frequency region on dielectric properties of sintered mullite ceramics at various heating rates: (a) 5 °min^{-1} and (b) 30 °min^{-1}.

Moreover, the sintering temperature weakly affects the dielectric properties as shown in Fig. 8. The most remarkable result is that the dielectric permittivity ($\acute{\varepsilon}$) is essentially frequency dependent between the radiofrequency range in megahertz (a) and the microwave frequency range in gigahertz (b). In fact, such a surprising investigation exhibits better dielectric properties for the mullite sintered samples to be conducted under the continuous gigahertz frequency range.

Fig. 9 indicates the variation of dielectric loss (tan δ) as a function of sintering temperature at 1.5 GHz with different heating rates. It is observed that the dielectric loss

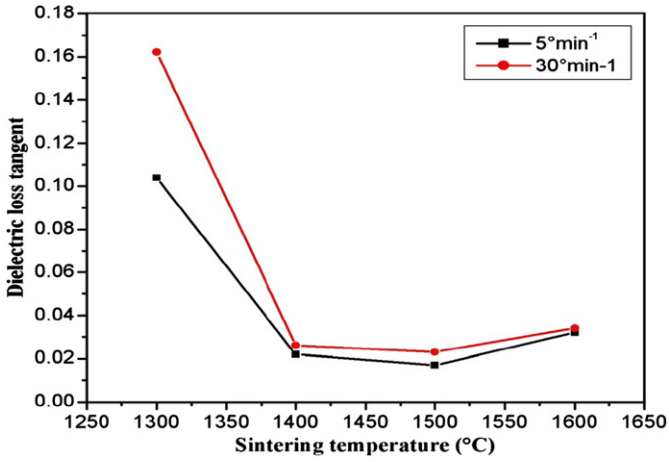

Fig. 9. Dependence of dielectric loss tangent (tan δ) of mullite samples on the heating rate and sintering temperature at 1.5 GHz.

decreased with increasing sintering temperature up to 1400 °C, as saturation is obtained above 1400 °C. It is known that the dielectric loss tangent tan δ is a dimensionless ratio of the imaginary dielectric loss to the real dielectric loss, tan $\delta = \varepsilon''/\varepsilon'$. Therefore, slowing the heating rate of the sintering process positively affects the dielectric properties of the mullite sintered samples, particularly in the gigahertz frequency range (i.e. decreases the imaginary part dielectric permittivity, ε'').

4. Conclusion

Single phase nanocrystalline mullite powders prepared from alkaline monophasic salts have been sintered at different temperatures from 1300 to 1600 °C under two heating rates, 5° and 30 °min^{-1}. The maximum bulk density of mullite samples obtained at the slow heating rate was about 2.65 g/cm^3 at the sintering temperature 1500 °C. Mullite samples sintered under slow heating rate over the temperature range have high values of microhardness compared with those sintered under the fast heating rate. Clear differences were found in the microstructures of mullite samples that could be related to the change in heating rate, which have an apparent effect on the densification behavior. Furthermore, it was found that mullite composites sintered at 1600 °C under the fast heating rate have a duplex DC resistivity value compared with those prepared under slow heating rate. The dielectric permittivity measurements of the prepared mullite nanopowders exhibited high values through sintering under the fast heating rate. A strong dependency of the dielectric permittivity on the frequency was observed for all the samples. According to the dielectric loss results, the sintering temperature was found to be a small impact after 1400 °C. Furthermore, the effect of heating rate on the dielectric loss could be observed either in the radiowave frequency region or in the microwave frequency region.

References

[1] H. Schneider, J. Schreuer, B. Hildmann, Structure and properties of mullite—a review, Journal of the European Ceramic Society 28 (10) (2008) 329–344.
[2] N.M. Rendtorff, L.B. Garrido, E.F. Aglietti, Mechanical and fracture properties of zircon–mullite composites obtained by direct sintering, Ceramics International 35 (7) (2009) 2907–2913.
[3] P. Sarin, W. Yoon, R.P. Haggerty, C. Chiritescu, N.C. Bhorkar, W.M. Kriven, Effect of transition metal ion doping on high temperature thermal expansion of 3:2 mullite—an in situ high temperature, synchrotron diffraction study, Journal of the European Ceramic Society 28 (2008) 353–365.
[4] F.A. Costa Oliveira, V. Livramento, F. Delmas, Novel mullite-based ceramics manufactured from inorganic wastes: II: mechanical behavior, Journal of Materials Processing Technology 195 (1–3) (2008) 255–259.
[5] H. Kalkanci, S.C. Kurnaz, The effect of process parameters on mullite-based plasma electrolytic oxide coatings, Surface and Coatings Technology 203 (2008) 15–22.
[6] T. Ebadzadeh, Formation of mullite from precursor powders: sintering, microstructure and mechanical properties, Materials Science and Engineering A355 (2003) 56–61.
[7] Jian Yu, Jian-Lin Shi, Qi-Ming Yuan, Zheng-Fang Yang, Yu-Ru Chen, Effect of composition on the sintering and microstructure of diphasic mullite gels, Ceramics International 26 (2000) 255–263.
[8] T. Ebadzadeh, Effect of mechanical activation and microwave heating on synthesis and sintering of nano-structured mullite, Journal of Alloys and Compounds 489 (2010) 125–129.
[9] Manas K. Haldara, G. Banerjee, Properties of zirconia–mullite composites prepared from beach sand sillimanite, Materials Letters 57 (2003) 3513–3520.
[10] MA Bei-yue, LI Ying, CUI Shao-gang, ZHAI Yu-chun, Preparation and sintering properties of zirconia-mullite-corundum composites using fly ash and zircon, Transactions of the Nonferrous Metals Society of China 20 (2010) 2331–2335.
[11] M.A. Camerucci, G. Urretavizcaya, A.L. Cavalieri, Mechanical behavior of cordierite and cordierite–mullite materials evaluated by indentation techniques, Journal of the European Ceramic Society 21 (2001) 1195–1204.
[12] J. Roy, N. Bandyopadhyay, S. Das, S. Maitra, Effect of CoO on the formation of mullite ceramics from diphasic Al_2O_3–SiO_2 gel, Journal of Engineering Science and Technology Review 3 (1) (2010) 136–141.
[13] L. Montanaro, C. Perrot, C. Esnouf, G. Thollet, G. Fantozzi, A. Negro, Sintering of industrial mullites in the presence of magnesia as a sintering aid, Journal of the American Ceramic Society 83 (1) (2000) 189–196.
[14] Y. Dong, J. Zhou, B. Lin, Y. Wang, S. Wang, L. Miao, Y. Lang, X. Liu, G. Meng, Reaction-sintered porous mineral-based mullite ceramic membrane supports made from recycled materials, Journal of Hazardous Materials 172 (2009) 180–186.
[15] S. Maitra, A. Rahaman, A. Sarkar, A. Tarafdar, Zirconia–mullite materials prepared from semi-colloidal route derived precursors, Ceramics International 32 (2006) 201–206.
[16] E. Tkalcec, D. Hoebbel, R. Nass, H. Schmidt, Structural changes of mullite precursors in presence of polyetheleneimine, Journal of Non-Crystalline Solids 3–4 (1999) 233–243.
[17] J. Roy, N. Bandyopadhyay, S. Das, S. Maitra, Role of V_2O_5 on the formation of chemical mullite from aluminosilicate precursor, Ceramics International 36 (2010) 1603–1608.
[18] C.Y. Chen, G.S. Lan, W.H. Tuan, Preparation of mullite by the reaction sintering of kaolinite and alumina, Journal of the European Ceramic Society 20 (2000) 2519–2525.
[19] H.C. Park, T.Y. Yang, S.Y. Yoon, R. Stevens, Preparation of zirconia–mullite composites by an infiltration route, Materials Science and Engineering A 405 (2005) 233–238.

[20] C. Aksel, The role of fine alumina and mullite particles on the thermo-mechanical behaviour of alumina–mullite refractory materials, Materials Letters 57 (2002) 708–714.
[21] S. Maitra, S. Pal, S. Nath, A. Pandey, R. Lodha, Role of MgO and Cr_2O_3 additives on the properties of zirconia–mullite composites, Ceramics International 28 (2002) 819–826.
[22] Y.M.M. AL-Jarsha, H.G. Emblem, K. Jones, M.A. Mohd. Abd. Rahman, Preparation, characterization and uses of mullite grain, Journal of Materials Science 25 (1990) 2873–2880.
[23] J. Meng, S. Cai, Z. Yang, Q. Yuan, Y. Chen, Microstructure and mechanical properties of mullite ceramics containing rodlike particles, Journal of the European Ceramic Society 18 (1998) 1107–1114.
[24] E. Mouchon, P. Colomban, Microwave absorbent: preparation, mechanical properties and r.f.-microwave conductivity of SiC (and/or mullite) fibre reinforced Nasicon matrix Composites, Journal of Materials Science 31 (1996) 323–334.
[25] R.A. Gerhardt, Volume fraction and whisker orientation dependence of the electrical properties of SiC-whisker-reinforced mullite composites, Journal of the American Ceramic Society 84 (10) (2001) 2328–2334.
[26] F. Cipri, C. Bartuli, T. Valente, F. Casadei, Electromagnetic and mechanical properties of silica-aluminosilicates plasma sprayed composite coatings, Journal of Thermal Spray Technology 5–6 (2007) 831–838.
[27] M.A. Camerucci, G. Urretavizcaya, M.S. Castro, A.L. Cavalieri, Electrical properties and thermal expansion of cordierite and cordierite–mullite materials, Journal of the European Ceramic Society 21 (2001) 2917–2923.
[28] N. El-Kadry, A. Aahour, S.A. Mohamoud, Structural dependence of DC electrical prperties of physically deposited Cd–Te thin films, Thin Solid Films 269 (1–2) (1995) 112–116.
[29] S. Li, N. Li, Influences of composition of starting powders and sintering temperature on the pore size distribution of porous corundum–mullite ceramics, Science of Sintering 37 (2005) 173–180.
[30] M.K. Haldar, Effect of magnesia additions on the properties of zirconia–mullite composites derived from sillimanite beach sand, Ceramics International 29 (2003) 573–581.
[31] S.H. Hong, G.L. Messing, Anisotropic grain growth in diphasic- gel-derived titania-doped mullite, Journal of the American Ceramic Society 81 (1998) 1269–1277.
[32] F. Kara, J.A. Little, Sintering of pre-mullite powder obtained by chemical processing, Journal of Materials Science 28 (1993) 1323–1326.
[33] M.G.M.U. Ismail, Z. Nakai, S. Somiya, Microstructure and mechanical properties of mullite prepared by the sol–gel method, Journal of the American Ceramic Society 70 (1987) C7.
[34] D.-G. Kim, G.-S. Kim, M.-J. Suk, S.-T. Oh, Y.D. Kim, Effect of heating rate on microstructural homogeneity of sintered W–15 wt% Cu nanocomposite fabricated from W–CuO powder mixture, Scripta Materialia 51 (2004) 677–681.
[35] J. Yu, J.-L. Shi, Q.-M. Yuan, Z.-F. Yang, Y.-R. Chen, Effect of composition on the sintering and microstructure of diphasic mullite gels, Ceramics International 26 (2000) 255–263.
[36] S.-H. Hong, W. Cermignani, G.L. Messing, Anisoptropic grain growth in seeded and B_2O_3-doped diphasic mullite gels, Journal of the European Ceramic Society 16 (1996) 133–141.
[37] S.-H. Hong, G.L. Messing, Anisotropic grain growth in diphasic gel-derived titania-doped mullite, Journal of the American Ceramic Society 81 (1998) 1269–1277.
[38] D.W. Richerson, Modern Ceramic Engineering: Properties, Processing, and Use in Design, Marcel Dekker, Inc., New York, 1982.